Structural Engineering and Mechanics, Vol. 9, No. 3 (2000) 289-304
DOI: http://dx.doi.org/10.12989/sem.2000.9.3.289

Experiments and analysis of the post-buckling behaviors of aluminum alloy double layer space grids applying ball joints

Yujiro Hiyama†

Sumitomo Light Metal Industries Ltd., 4-1-23, Heiwajima, Ohta-ku, Tokyo 143-0006, Japan

Koichiro Ishikawa‡

Department of Architecture and Civil Engineering, Fukui University, 3-9-1 Bunkyo, Fukui-shi 910-8507, Japan

Shiro Kato†‡

Department of Architecture and Civil Engineering, Toyohashi University of Technology, 1-1 Tempaku-cho, Toyohashi-shi 441-8122, Japan

Shoji Okubo‡‡

Sumitomo Light Metal Industries Ltd., 4-1-23, Heiwajima, Ohta-ku, Tokyo 143-0006, Japan

Abstract. This study discusses on the experimental and analytical results of the global buckling tests, carried out on aluminum alloy double layer space grids composed of tubular members, ball joints and connecting bolts at the member ends, with the purpose of demonstrating the effectiveness of a simplified analysis method using an equivalent slenderness ratio for the members. Because very few experiments have been carried out on this type of aluminum space grids, the buckling behavior is investigated experimentally over the post buckling regions using several space grid specimen with various values for the member slenderness ratio. The observed behavior during the experiments is compared with the analytically obtained results. The comparison is made based on two different schemes; one on the plastic hinge method considering a bending moment-axial force interaction for members and the other on a method using an equivalent slenderness ratio. It is confirmed that the equivalent slenderness method can be effectively applied, even in the post buckling regions, once the effects of the rotational rigidity at the ball joints are appropriately evaluated, because the rigidity controls the buckling behavior. The effectiveness of the equivalent slenderness method will be widely utilized for estimation of the ultimate strength, even in post buckling regions for large span aluminum space grids composed of an extreme large number of nodes and members.

Key words: space grids; ball joints; aluminum; buckling behavior.

† Chief Engineer
‡ Associate Professor
†‡ Professor
‡‡ Engineer

1. Introduction

The usage of aluminum alloys as structural materials in the building industry has increased steadily owing to advantageous material properties, such as primarily a high strength to weight performance and corrosion resistance. Aluminum alloys, with a strength equivalent to steel and a characteristic low specific gravity are suited for realization of large span structures. For the same reasons aluminum alloys can be put to an effective use for structural members in walls, separation walls, cladding etc, ultimately resulting in a beneficial reduction of dead load on the building foundations. However, aluminum alloys do have some unfavorable material characteristics such as a high yield ratio and a decrease in strength after welding, caused by inherent properties of heat-treated alloys. This reduction in strength is a significant design parameter. Therefore, the structural design for aluminum alloys should be executed in consideration with the material behavior after yielding and with a proper evaluation of the ultimate strength in each aluminum component.

The present paper focuses on double layer space grids at present widely used for metal roofs, with the aim of researching the feasibility of aluminum for usage in such space grids, because of its seemingly higher effectiveness for realization of light weight architecture than the use of steel. The global structural behavior in this kind of structures is strongly governed by nonlinear buckling in the members and the connecting system and accordingly this study considers the nonlinear behavior of the space grids, including buckling of members, each consisting of one aluminum tubular element and two ball joints at the connections.

The structural calculation in the design of the double layer space grids have generally treated the connections as pin joints and as a result the global buckling strength of the space grid was underestimated unless the members in tension did not yield. However, as explained in Hiyama, Takashima, Iijima and Kato (1997), the type of connection here used is considered to provide some bending stiffness and therefore the actual buckling strength is expected to exceed the theoretical value for idealized pin joints. Such an underestimation of the member buckling strength relative to the reduced tensile axial strength, does not always lead to a safer design, because the yielding in tension members will actually occur different from the condition where under the designers assume buckling in axial members in the initial design.

Therefore this research will present the experimental results obtained from the buckling behavior tests of the space grids using aluminum ball joints for the connections and will investigate the effective member slenderness ratio corresponding to the actual buckling strength of the composing members. From the results of the buckling tests, the post-buckling behavior of the truss member relative to the member slenderness ratio is evaluated in accordance with past researches made into steel by Saka and Heki (1984), El-Sheikh (1998). Buckling analyses follow the tested structural models, making use of two modeling methods together with a discussion of the accuracy of the analytical methods simulating the structural tests. Furthermore, using one of the two modeling methods, the buckling analyses are performed on a flat large scaled double layer space grid which could practically be constructed and the numerical efficiency of the above non-linear analysis for such large scaled double layer space structures is evaluated.

2. Loading test for the unit space grid

A full scale loading test of the simple beam type was executed and a proportional and cyclic

loading was applied to the unit space grids in order to investigate the buckling characteristics of the truss members with different member slenderness ratios.

2.1. Specimen and test method

Fig. 1 illustrates the aluminum alloy truss connections and denotes the material standards used in this study. The members called “struts” are tubular members. A conical fitting called “end plug” is welded to either end of the “struts”. In advance a bearing bolt is inserted into a bolt hole at the center of the cross section of the end plug. A retaining pin is inserted into the bearing bolt in the cross sectional direction just outside the end plug and enters the grooves in the pipe-shaped collar. The strut is connected to the solid ball, called the “hub”, by rotating the collar and screwing the bearing bolt to designated drill hole of the hub.

All the applied struts, hubs, collars, and end-plugs are fabricated of extruded aluminum 6061-T6, Al-Mg-Si heat-treated alloy. The bearing bolts are high tension bolts made of Cr-Mo quenched and annealed steel. Table 1 shows the constitutive members and their sectional properties. A total of five specimen with different member slenderness ratios are prepared.

Fig. 2 summarizes the experimental set-up of the buckling tests and measurements. The tightening torque of the collar is set at 29.4Nm. Two of the outer hubs are fixed and the other two hubs are

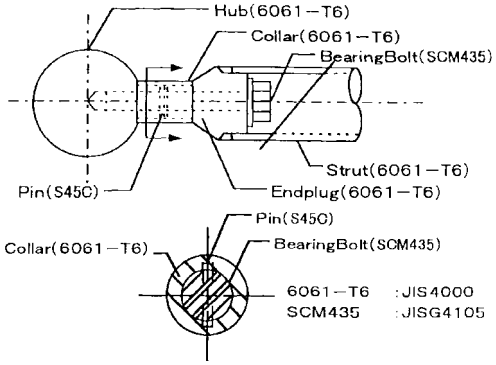

Fig. 1 Configuration and material standards of aluminum alloy truss connections

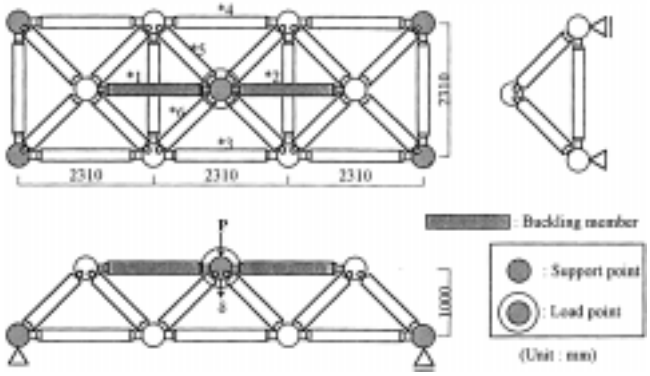

Fig. 2 Truss beam for buckling tests and analyses (For all the upper chords member type S1 to S5 are used and for all the lower chords and diagonal members type S6 is used.)

Table 1 Specimen used for buckling tests of the space-grid, theoretical buckling stress σ^{U}_{cr} and experimental buckling stress σ^{E}_{cr}

specimen	Strut	Bolt	Collar	Hub	*Kb* (kN · cm/rad)	λ/Λ	σ^{U}_{cr} (MPa)	σ^{E}_{cr} (MPa)
S1	Φ 63.5 × t6.35	M20	Φ40	Φ228	4.78	1.40	54	99, 101
S2	Φ 63.5 × t2.5	M16	Φ32	Φ228	2.11	1.32	60	105, 105
S3	Φ 88.9 × t7.6	M27	Φ54	Φ228	11.45	0.99	105	169, 169
S4	Φ100.0 × t7.0	M27	Φ54	Φ228	11.45	0.86	129	198, 185
S5	Φ114.3 × t10.9	M33	Φ66	Φ228	22.50	0.77	146	240, 243
S6	Φ141.3 × t12.7	M39	Φ78	Φ228	37.18	0.62	149	---------

roller supported allowing for movement horizontally in longitudinal direction. The upper two chords of the space grids in Fig. 2 are the members, in which member buckling was observed and correspond to S1 through S5 specimen as listed in Table 1.

The buckling tests were carried out in succession, exchanging the upper two chords for members with different slenderness ratios and investigating the respective buckling strength and post-buckling behavior. All the lower chords and the diagonal lattices, except for the two upper chords, are coded S6 in Table 1. They were designed in such a way that the yielding in tension or compression (buckling) would not occur until the objective upper chords reached the buckling loads in the experiments.

The theoretical buckling stress σ^{U}_{cr} for the different specimen is calculated based on the following general formulas and is also shown in Table 1. In the case of the elastic buckling region of $\lambda / \Lambda \geqq 1$, σ^{U}_{cr} is calculated by using Euler's buckling formula defined as $\sigma^{U}_{cr} = \pi^2 E / \pi^2$, where is the member slenderness ratio calculated by = L_k/i, wherein i is the radius of gyration and L_k is the unsupported length. In this study, L_k is taken to be 231 cm of the distance between the two nodes. E is the Young's modulus of 710^4 N/mm^2 for aluminum alloy. The critical slenderness ratio, defined as $\Lambda = \sqrt{\pi^2 E / \sigma^{\lim}_{cr}}$, is calculated to be 80, supposing the ratio of the elastic limit stress for the Euler's buckling to the basic value F, expressed by $\sigma^{\lim}_{cr}/F$, is taken 0.5 or $\sigma^{\lim}_{cr} = 0.5F$. F is the basic value of the yield stress of 6061-T6 alloy for structural design and is assumed 210 N/mm^2. In the case of elasto-plastc buckling region of $\lambda/\Lambda < 1$, the relation between σ_{cr} and λ is assumed to keep a linear relationship between the stress and strain until the stress reaches the $0.5F$ and is limited not to exceed the yield stress F_w of the welded parts. F_w is assumed to be 149 N/mm^2 for the 6061-T6 alloy by the method of the friction welding and the ratio to the basic value F is 0.71. 149 N/mm^2 is the basic value of the yield stress for the design whose numerical value is usually used for this way of welding.

In Table 1, the parameters of the experiment are the member slenderness ratio λ and the objective value of the λ/Λ are 0.77 to 1.40 as centered in specimen S3 whose λ is approximately equal to the critical slenderness ratio Λ. This is because Λ is usually used as the λ of the chords, forming a balance between the unit length and the span length in the actual design for the double layer space grids. The elastic bending stiffness of the connections K_b (KNcm/rad) obtained from author's previous research as explained in Hiyama, Takashima, Iijima and Kato (1997) is also noted for each specimen in Table 1. The value of K_b, defined as $M = K_b\phi$, where M is the bending moment and ϕ is the rotational angle, was investigated through bending test of a simple supported beam by the following procedure. The connection was set up in the center of the beam of specimen and the concentrated loading was applied to the connections. The K_b was obtained from the relation

Table 2 Mechanical properties of components

Components	σ_y (MPa)	σ_u (MPa)	Elongation (%)
Strut	252	306	15
Bearing Bolt	-	911	-
Collar	281	315	17
End-plug	269	313	17
Hub	301	339	19
Welded Part	162	225	13

between the applied bending moment M and the measured rotational angle ϕ that the theoretical center displacement assuming the continuity of the strut between the supports (no joint exists) is subtracted from the observed value of central displacement and the resultant displacement is converted into the rotational angle ϕ. The more detailed explanation is stated in Hiyama *et al.* (1997).

The bending stiffness of the connections κ normalized by the bending stiffness of the member and expressed as EI/l, is 1.15 to 3.36. This value for κ can be evaluated as the semi-rigidity for the joints as used in many previous researches made into single layer latticed shells as example in Ueki, Mukaiyama, Shomura and Kato (1991).

Table 2 shows the measurement value of the material properties for the components of the specimen. The yield stresses σ_y and the ultimate strength σ_u are the average of six measurements from S1 to S6, subtracting double standard deviation 2Sx from the average value. In Table 2, the yield ratio defined as σ_y/σ_u of all aluminum alloy components shows a high value of almost 0.85 on the average. These results indicate that the material is not expected to resist further after material yielding. “Welded part” expresses the values of the welded connection for the joint between strut and end-plug using friction welding as mentioned before. The minimum and maximum stress for σ_y is 160 and 178 N/mm^2, further for σ_u 218 and 243 N/mm^2 respectively for the welded parts. Because the differences between the minimum and maximum stresses indicate only about 10%, friction welding is apparently a suitable method for the welding of the aluminum tubes.

A vertical load was applied to the center hub of the space grid by using a 500KN hydraulic jack fixed to the reaction frame setting on the test bed. Two specimen (upper chords) were prepared and the testing procedure for each specimen was programmed as follows: (1) Loads were applied until the buckling of the objective upper chords was reached; (2) After the buckling, loads were cyclically applied from two to four cycles until the relation between load and displacement showed nearly horizontally.

The cyclic loading in the test procedure (2) was carried out supposing the following behavior of the buckling member against the seismic cyclic loading. First, if one member reaches the maximum strength in buckling, a reduction of the axial stiffness of the buckling member results and re-distribution of the member forces occurs over the whole of the space grids. Accordingly, in case of seismic cyclic loading, the deformation of the buckling member may not progresses momentarily, the buckling member can be expected to absorb the seismic force by the retained post-buckling strength.

The displacement for the loading hub was measured vertically and for the unsupported hubs of the lower chords vertically and horizontally, by means of dial gauges. The strains on the members were measured on four sides of the cross sections of the members as denoted by the star marks in Fig. 2.

Table 3 Comparison between experiments and analyses for axial forces in the elastic range

specimen	experiments			analyses			experiments/analyses		
	upper	lower	diago.	upper	lower	diago.	upper	lower	diago.
S1	-1.14	0.88	-0.44	-1.09	0.85	-0.49	1.04	1.04	0.90
S2	-1.10	0.84	-0.51	-1.02	0.84	-0.51	1.08	1.00	1.00
S3	-1.16	0.87	-0.49	-1.12	0.85	-0.48	1.04	1.02	1.02
S4	-1.15	0.85	-0.46	-1.12	0.85	-0.48	1.03	1.00	0.96
S5	-1.02	0.84	-0.45	-1.13	0.85	-0.47	0.90	0.99	0.96

For upper chords *1 and *2 of the observed buckling members, the strain gauges were fixed at both ends and in the center of the members, because of the expected formation of a plastic hinge in the case of buckling.

2.2. Discussion of test results

Table 3 describes the axial forces of the members *1, *3 and *6 respectively, for the upper, lower chords and the diagonal lattices (see also Fig. 2) normalized by a unit load of 1.0 KN in the elastic region. A comparison is made between the experimental results obtained from the strain at the center of the strut and analyses assuming their connections as a pin joint. Each specimen shows relatively good agreement, that is, the ratio of experiments to analyses indicates 0.90 to 1.08, however, it may be necessary to refine the experiments to accumulate more reliable data.

The buckling stress σ_{cr}^{E} for the two chord members obtained from the test results is shown in Table 1 together with the theoretical buckling stress being σ_{cr}^{U}. Further, Fig. 3 shows the relationships between the applied load P measured by a loading cell and the vertical displacement of the loading hub for specimen S1 to S5. The applied load P is normalized by the theoretical buckling load P_{cr}^{U} of the space grid, when the axial stress in the upper chords becomes the theoretical buckling stress σ_{cr}^{U}. Also the displacement δ is normalized by δ_{cr}^{U} being the elastic theoretical displacement in the theoretical buckling load P_{cr}^{U}.

In Fig. 3, all the specimen experience nearly linear behaviors until the buckling load level, beyond which a sudden loss of strength occurs down to a low residual level. Furthermore a substantial

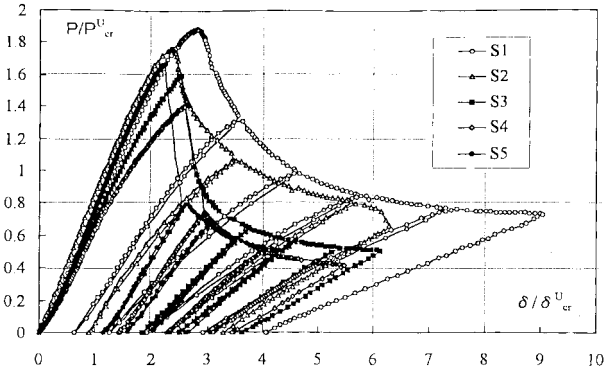

Fig. 3 Relationships between the applied load P and the vertical displacement δ of the loading hub for specimen S1 to S5

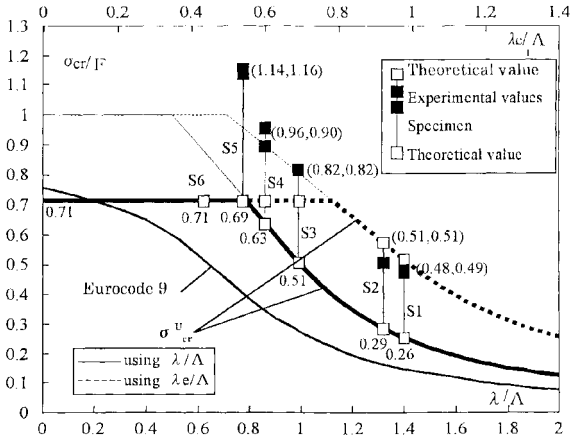

Fig. 4 Relationship between buckling stress σ_{cr}^{E} of the experimental results and the slenderness ratio λ, compared to the theoretical buckling stress σ_{cr}^{U}, where λ_e=0.7×λ, Λ=80 and F=210 MPa

sudden loss is observed, in the case of member type S3, S4 and S5 all with a slenderness ratio smaller than the critical slenderness ratio. It is well known that a similar sudden critical loss occurs in this kind of steel members with $\lambda/\Lambda \leqq /1.0$.

Fig. 4 shows the relationship between the buckling stress σ_{cr}^{E} and the member slenderness ratio λ, compared to the theoretical buckling stress σ_{cr}^{U} discussed in details in section 2-1. Furthermore, the buckling stress defined by Eurocode 9 (1997), as a typical buckling formula for the aluminum structural design, is also plotted together in Fig. 4. The buckling stress of Eurocode 9 indicates almost 0.7 times that of σ_{cr}^{U}, because the formula considers a safety factor to be the design code.

With regard to the buckling stress in Fig. 4, the experimental values of S1 and S2, for which λ is larger than Λ, are 1.88 and 1.76 times the theoretical values. Similarly S3, S4 and S5, for which λ is smaller than Λ, are 1.58, 1.31 and 1.66 times the theoretical values, respectively. In other words, the experimental values for the buckling stress showed about twice the theoretical value in the region of the Euler's buckling load.

Next, to find the elastic buckling mode, the eigenvalue analysis was executed for the members of the specimen, considering the bending stiffness *Kb* (KNcm/rad) of joints in Table 1, obtained from the experimental research in Hiyama *et al.* (1997). The effective slenderness ratio λ calculated from the equivalent buckling length l_k^{lin} given by Eq. (1) using Euler's buckling formula, were determined to be 0.68 to 0.78 (0.73 on the average) of the slenderness ratio λ derived from the nominal length of the truss member.

$$l_k^{lin} = \sqrt{\frac{\pi^2 EI}{P_{cr}^{lin}}} \tag{1}$$

wherein P_{cr}^{lin} is taken as the analyzed buckling force of the eigenvalue analyses. *E* and *I* denote the Young's modulus of aluminum (710^4 N/mm^2) and the moment of inertia of the struts.

On the other hand, in the case of elastic buckling region of $\lambda/\Lambda \geqq 1$, the experimental values were closed to the theoretical buckling curve when the experimental buckling force was plotted at the position 0.7 times λ/Λ as illustrated in Fig. 4. As a result, taking into consideration of the results of the eigenvalue analyses, it may be quite possible to consider the effective slenderness ratio λ_e as 0.7 λ. In the case of elasto-plastic buckling region of λ/Λ <1, experimental values do not

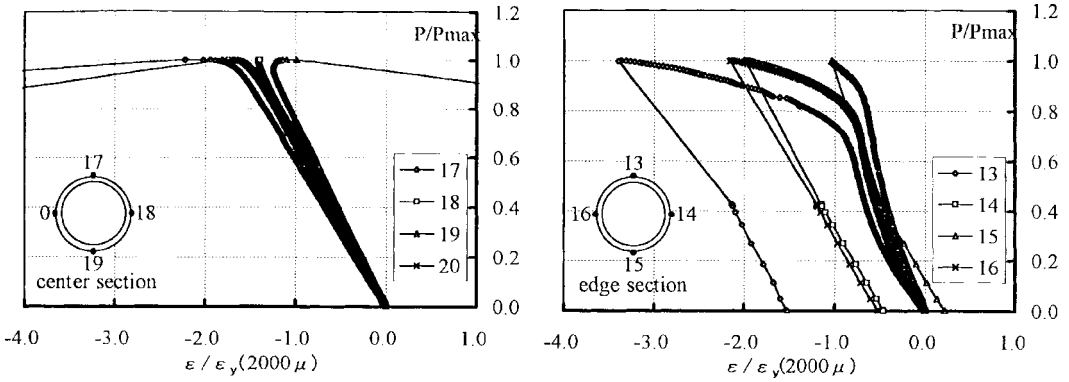

Fig. 5 Relationship between the applied load P and the strain ε of the upper chord for specimen S5

have a good agreement with the calculated buckling stress using a formula of a design code. It may be understood by the following reasons: (1) the theoretical buckling stress σ_{cr}^{U} is formulated on the safety side, which reflects on deriving the critical slenderness ratio λ_e using 0.5F; (2) as mentioned later, the welded section did not reach the local buckling because the shape of the tube section was restrained with the end-plug at the end of the member.

When the relationship between load and displacement deviated from linearity, the specimen (upper chords) began to swell in the welded parts at the ends of the members. Then, the maximum strength appeared in the process of buckling. After that, the load decreased because of deflection of the buckling member into out of plane direction. During cyclic loading, there were no significant progressive failures neither in the welded sections nor in the center of the members after the maximum strength was reached.

Fig. 5 plots the observed results of the strain measurments in the center part and the welded part of the member for specimen S5 whose theoretical buckling stress is close to the yield stress of the welded part. The values of four strains fixed to the cross-section in the center part were constantly increased in compressive direction. When the measured strain had reached around 1.2 times the theoretical yield strain of 0.2%, some of the strains were turned into the tensile direction and a remarkable increase was observed. On the contrary, all of the strains of the welded part constantly increased into compressive direction without rapid change until the buckling load was reached. The maximum strain to the yield strain for the welded part was 2.0 on the average. This phenomena of a high srength for the welded parts is considered to be caused by a constraint from deformation resulting from the end-plug. As a result, it can be considered that there is almost no reduction in effective srength for such a welding condition. The other four specimen indicated almost the same behavior. From the above observed strain for the upper chord, it is cleary seen that the local buckling and also the bearing collapse did not occur at the welded part and that the member buckling precedently happened in the elasto-plastic buckling region.

The effective slenderness ratio λ_e discussed in this chapter was investigated by using the assumption that the buckling length would be influenced mainly by the bending stiffness of the connection because the rotation of the connection is almost restrained by the large size diagonal struts jointed the objective connections. However, when the span of the space grid is so long and the bending moments exceed the shearing forces, the sectional area of the diagonal struts become small. Therefore, in the case of such model and member configurations of space grid, the effective slenderness ratio λ_e obtained from the present buckling test might be slightly overestimation.

Accordingly, on the precision of the buckling strength calculated by using this λ_e and the applicability, further experimental studies for the different joining condition or for the specimen with different nos. of connecting struts and different connecting angles would be necessary in future. However, for the space grid having common member constitutions and relation of unit size and depth, the proposed calculation method by using this λ_e would predict approximately the buckling strength of the member.

3. Numerical simulation

The elasto-plastic buckling analyses were executed, considering the effects of geometric and material non-linearity of the members, by using two kinds of analytical modeling, such as the beam-column and the truss elements model. The purpose of the analyses is to compare analytical and experimental results concerning the elastic rigidities, buckling loads and post-buckling behavior of these space grids and to propose the proper analytical method with which the actual behavior for such space grids can be simulated.

3.1. Analytical method

3.1.1. Beam-column elements assuming rotational springs and rigid zones at both ends (analytical method A)

In the analytical modeling of the tubular aluminum members, the following assumptions are used. As shown in Fig. 6, each truss member is composed of three kinds of analytical elements such as an elastic spring element for axial and bending actions at the both ends connections, an elasto-plastic spring element for the elasto-plastic deformation of the middle point and two ends and an elastic beam-column element between the springs.

The formulation of the elastic stiffness for the elastic beam-column elements in the model is based on a stability slope-deflection method.

The elasto-plastic elements are assumed to behave elastically up to the yield point. Thereafter, the elements are assumed to flow plastically with the axial force N and bending moments M_Y and M_Z (with respect to the y and z axes, respectively) constrained to the yield surface defined by the following equation:

$$f=\left(\frac{N}{N_Y}\right)^2+\sqrt{\left(\frac{M_y}{M_P}\right)^2+\left(\frac{M_z}{M_P}\right)^2}=1 \tag{2}$$

In Eq. (2), N_Y is the axial yield force and M_P is the full plastic moment. The more detailed

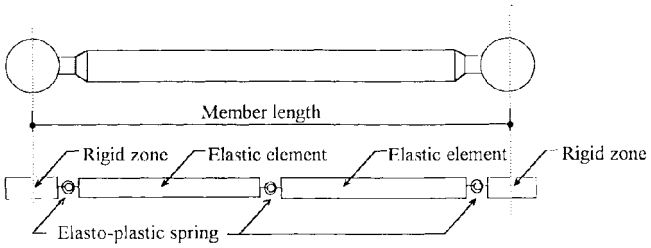

Fig. 6 Elasto-plastic beam-column element for analytical method A

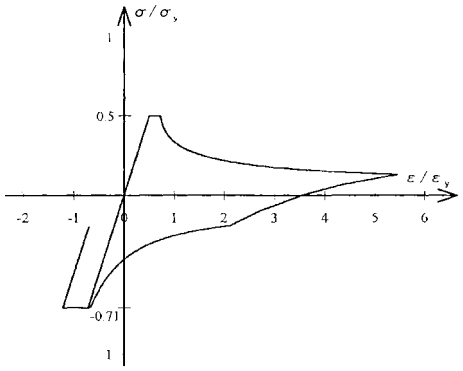

Fig. 7 Model of a pin-jointed member under loading in the case that λ/Λ=1.0

explanation is stated in Ueki, Mukaiyama, Shomura and Kato (1991).

The connection springs at the both ends of the each member are assumed to remain in the elastic region, because the connections are considered to have more strength in comparison with other elements in the member.

In the case rigid connections, the rigidities of those springs are set large enough to be considered rigid. And in the case of semi-rigid and strong connections, the rigidities are set corresponding to experiments or analyses (Kato and Murata 1997).

3.1.2. Truss elements assuming pin-jointed member buckling under axial load (analytical method B)

The other modeling of the members assumes that the members constitute a pin-connected truss element. This model adopts the assumption that the member buckle due to compression and yield under tension. Fig. 7 shows the hysteresis curves in the case of a member slenderness ratio of λ/Λ =1.0 as an example. The maximum compressive stress σ_{CR} of the members is calculated by the formula stated in section 2-1. The effects of the initial imperfection contained in the members is considered by deriving the critical slenderness ratio λ using the proportional limit stress of the elastic buckling 0.5*F*.

The hysteresis curves are obtained by the present author's research, based on the formulation by Hagginbotham and Hanson (1976). The present study of the hysteresis adopts a plastic hinge concept, which includes secondary effects due to lateral displacements without strain hardening and also includes the plastic axial deformations at a hinge together with the elastic member shortening. The hysteresis rules for cyclic deformations are determined in the following manner. Two main curves, upper and lower, are approximated by two fully quadratic equations in terms of the stress and strain. And four straight lines are connected continuously with each other between the two main curves.

Based on the principle of minimum potential energy, the incremental stiffness matrix $[K_{Ti}]$ and the equivalent internal forces $\{F_i\}$ can be obtained. When every member is superimposed in the global equation for structures, the equilibrium equation is obtained and expressed symbolically by Eq. (3).

$$[K_{Ti}]\{D\} + \{F_i\} = \{P_{i+1}\} \tag{3}$$

where $\{D\}$ is the incremental displacement vector and $\{P_{i+1}\}$ is the external applied load at the time of time step i+1. For solving Eq. (3), Newton-Raphson iterative scheme is utilized (Ishikawa and Kato 1997).

Table 4 Assumed property for analyses

Specimens	S1	S2	S3	S4	S5
N_Y (kN)	234.6	98.6	399.5	420.9	698.0
M_P (kN·m)	4.29	1.92	10.37	12.49	24.07
Young's modulus (GPa)				70	
Yield-stress of Aluminum (MPa)				210	
Yield-stress for Aluminum welding (MPa)				149	

3.2. Comparison between analytical and experimental results for the unit space grid

3.2.1. Elasto-plastic buckling analysis using the beam column element model (analytical method A)

The elasto-plastic analyses of the unit space grids in Table 1 and Fig. 2 were carried out using the above mentioned beam column element method.

For the analyzed model of the space grids, the bending stiffness of the joints may be taken to be half the value of the initial stiffness as obtained in the experimental study dealing with this type of steel truss, see (Hagginbotham and Hanson 1976). The bending rigidity used for the analysis in this paper, is taken to be half the value of the initial stiffness as explained in Hiyama *et al*. (1997), because this assumption gives buckling loads close to those found experimentally.

The length of the rigid zone is assumed to be equal to the radius of the hubs. The axial yield force N_Y and the full plastic moment M_P of the member type S1 to S5 are shown in Table 4. The mechanical properties of the Young's modulus and yield stresses assumed for analyses are also shown in Table 4. The axial rigidity of the joints is taken to be 0.4×10^9N/m, which is an average value of compressive and tensile axial rigidities of the joints observed experimentally in the previous research concerning such aluminum joints.

The relationships between the applied load P and the vertical displacement δ at the central node of the space grid in Fig. 2, is obtained using this analytical method, applied to the trusses in case of four different configurations(S1 to S5 in Table 1) being used for the upper chords. The results of the two cases S1 and S2 are shown in Figs. 8 and 9. From the figures, it is seen that analytical and experimental values show a good agreement for the rigidities of initial and post-buckling stiffness

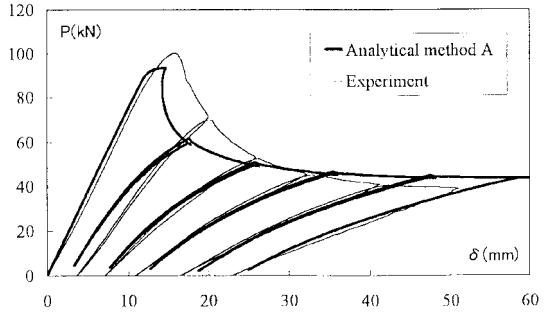

Fig. 8 Comparison of buckling curves between the analytical method A and the experiment in case of a truss beam with member type S1 for the upper chords

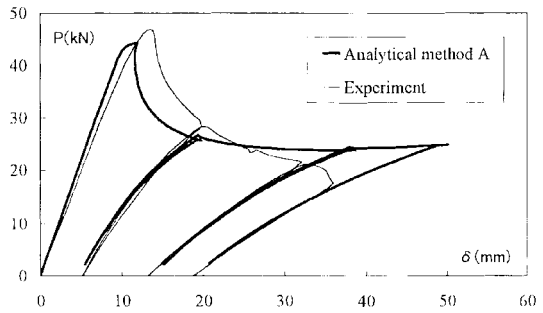

Fig. 9 Comparison of buckling curves between the analytical method A and the experiment in case of a truss beam with member type S2 for the upper chords

Table 5 Comparison of the maximum buckling loads of the space-grid with member type S1 to S5 for the upper chord obtained from the analytical method A and from the experiment

Member type for the upper chord	S1	S2	S3	S4	S5
Maximum strength by experiment (kN)	100.0	47.0	284.2	320.5	712.9
Maximum strength by analysis (method A) (kN)	93.1	44.1	258.7	301.8	570.9
Analytical value (method A)/Experimental value	0.93	0.94	0.91	0.94	0.80

and also show approximate agreement for deformation in the post-buckling region. Although not shown here, similar relationships were obtained through this analysis method for the other cases such as S3 to S5.

The buckling loads calculated by the analysis are much the same as the experimental buckling loads shown in Table 5. Accordingly, this analysis method can be regarded to provide a conservative estimation of the buckling loads of the trusses, because the ratio of the analysis to the experiment shows 0.93 on the average for S1to S4, excepting S5. The reason for the discrepancy of S5 is because the buckling stress in the experiment exceeded the yield stress σ_y of 210 N/mm^2 in Fig. 4, while the buckling stress is supposed to be restricted to σ_y in the analyses.

3.2.2. Elasto-plastic buckling analysis using the truss elements, incorporating member buckling (analytical method B)

An elasto-plastic buckling analysis of the space grids was carried out using the pin-jointed truss elements as mentioned above.

In this analysis, the cross-sectional areas of the members, which affect the rigidity of the space grids, are taken to be those of the struts. The effective slenderness ratios λ_e of the members are assumed to be 70 of the values of λ derived from the lengths between the two end nodes of the member. Based on the above mentioned investigations for the experimental buckling loads, the reduced slenderness ratio λ_e is evaluated.

Figs. 10 and 11 plot the relationships between the vertical load P and the vertical displacement at the center of the space grids in the two cases where the upper chord members are member type S1 and S2 compared to the experimental results, in the same way as analytical method A. It is seen that the analytical results such as the buckling loads and the buckling curves show good agreement

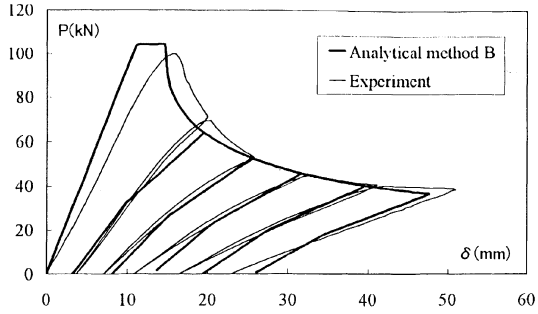

Fig. 10 Comparison of the buckling curves between the analytical method B and the experiment in case of a truss beam with member type S1 for the upper chords

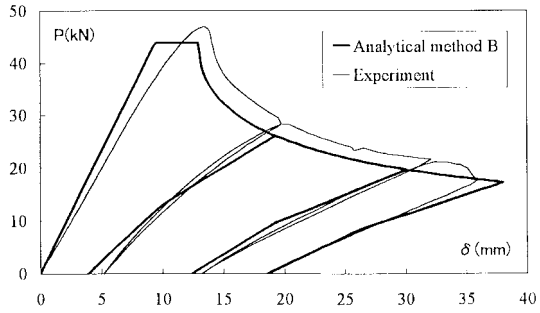

Fig. 11 Comparison of the buckling curves between the analytical method B and the experiment in case of a truss beam with member type S2 for the upper chords

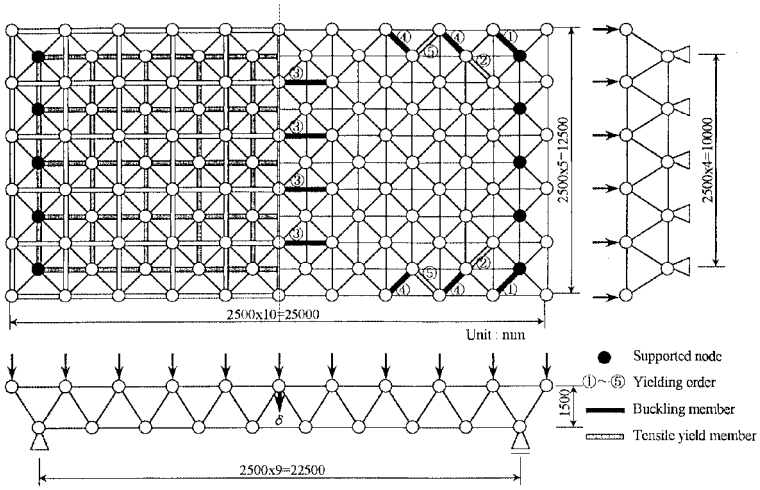

Fig. 12 Analyzed space grid

with those of the experiments. Accordingly, it could be confirm that analytical method B has an analytical precision about the same as the analytical method A.

4. Investigation of the collapse mode for an actual large scaled space grid

This section describes the implementation of the collapse analysis, using above mentioned analytical method B, on the example of the aluminum space grid to be designed for an actual large scale roof structure and discusses its expected collapse mode.

4.1. The objective space grids and the structural design

The objective roof structure composed of aluminum space grids, with dimensions of 25 m×12.5 m in plan is illustrated in Fig. 12. One space grid module measures 2.5×2.5 m in length and width and 1.5 m in depth. The supported span is 22.5 m or 9-modules in longitudinal direction and the supported hubs are fixed with pin supports on top of the cantilevered RC columns. In the structural calculation, the RC-column is regarded to have an infinite bending stiffness. The design loads are supposed as follows; 700 N/m^2 for the dead load including the roof finish, 3 KN/m^2 for the snow load calculated by the unit weight of 30 N/m^2/cm times a snow depth of 100 cm and 0.3G for the vertical seismic load. The constitutive members are calculated by σ^{U}_{CR} in section 2-1 with a yield stress of 210 N/mm^2. Also the yield stress for the welding part is limited to 149 N/mm^2. The member slenderness ratio λ for the member selection is considered to become close to 70 to 80.

The results of the structural design could be summarized as follows. Because the structure is mainly subjected to downward loading, the upper chord's compression and the lower chord's tensile force become the objective axial forces. In case of the buckling length supposed to be the length between the two end nodes of the member, the members selected are ϕ114.3×12.7 t, ϕ114.3×15.24 t and ϕ88.9×5.08 t for the upper, lower chords and the diagonal lattices respectively. The stress ratios for each buckling or tensile stress of the members are, for snow load as the main loading case, 0.73,

Table 6 Member properties for space-grid

Member	Strut	A (cm^2)	i (cm)	L_k (cm)	λ	λ/Λ	λ_e/Λ*1	Stress ratio*2
Upper	ϕ 114.3×t10.16	33.24	3.70	250	67.58	0.83	0.58	0.70
Lower	ϕ 114.3×t15.24	47.43	3.54	250	70.55	0.87	0.61	0.66
Diago.	ϕ 88.9×t3.81	10.19	3.01	232	76.99	0.95	0.67	0.74

*1 $\lambda_e=0.7\times\lambda$
*2 The stress ratio for buckling member are calculated as the ratio to the theoretical buckling stress by using λ_e

0.66 and 0.82, respectively. As a result, since the respective collapse mode would be the diagonal lattices first, then the upper chords and at last the lower chords in this order, the roof structure can be considered to avoid sudden collapse under an excessive load-condition larger than the pre-assumed design load. On the contrary, if the effective slenderness ratio $\lambda_e(0.7\lambda)$, which was investigated in the above mentioned experiments and analyses, is used for the calculation of the buckling stress of the members, the stress ratio of the upper chords would be 0.5 and the tensile collapse of the lower chords would be estimated at happening in advance. Therefore, the upper chords were exchanged to ϕ114×10.16 t or one profile lighter and also the diagonal lattices to ϕ88.9 ×3.81 t such that stress ratios modified to 0.70 and 0.74, making the collapse mode of the space grid as initially assumed. The section properties and the structural calculation results, for the above finalized members are shown in the Table 6.

4.2. Collapse mode by the elasto-plastic buckling analysis

The elasto-plastic buckling analyses were carried out on the above mentioned truss grids (see Fig. 12) by using analytical method B. The analyzed truss grid is composed of the verified members and its structural calculation was executed by using the effective slenderness ratio λ_e as mentioned in Table 6. The relationship between the uniform load P (KN/m^2) and the maximum vertical displacement at the center of the model is plotted in Fig. 13. The progression of the collapse mode is as follows: 1) The maximum load appeared at the buckling point of members－① and the tensile yield of members－② of the diagonal lattice; 2) After the re-distribution for the member forces of the space grid, the strength of the space grid increased again until the buckling of members－③ of the upper chords occurred; 3) After the buckling of member－③ the strength of the space grid

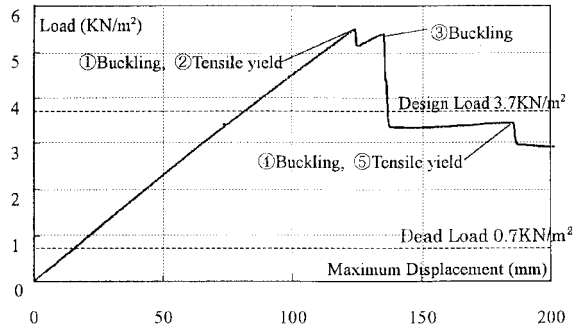

Fig. 13 Load-displacement relation calculated using analytical method B for the space grid roof structure

decreased to half the maximum strength; 4) Although the buckling of members –④ and the tensile yield of members – ⑤ of the diagonal lattices were occurred, the strength maintained almost horizontally and a sudden overall collapse cased by the tensile yielding of the lower chords did not occur.

As a result, the above mentioned analysis proved that the analyzed collapse mode is almost the same as the assumption of the structural design in section 4.1.

5. Conclusions

The present study aimed at investigating the buckling strength and post-buckling behavior of the space grid members connected with aluminum ball joints in a full-scale structural testing, based on the viewpoint that an underestimation of the buckling strength of the truss member is not necessarily a safe design. Showed were two analytical methods enabling the simulation of the buckling behavior for such space grids in the elastic-plastic region. Especially suited for large scale space grids, the pin-jointed equivalent modeling method, having an advantage in the computer performance, was proposed. Furthermore, the structural design and the elastic-plastic analysis with pin-jointed method was executed, targeting a large scale space grid roof structure that could actually be built. The objective for such structural design and analysis was to have enough ability of the plastic deformation occur over the whole of the space grid by giving priority to buckling in the compression members. From the above investigations, this research suggests that the proper evaluation of the buckling strength and behavior taking in consideration the rotational stiffness of the connections, is a problem one should not ignore.

The conclusions of the present study can be stated as follows:

1) The experiment confirmed that the tested truss member using aluminum ball joints showed almost the same pre-and post-buckling behavior in comparison to similar steel structures. Furthermore, it was confirmed that the reduction of the yield stress in the welds did not affect the buckling strength and the post-buckling behavior.

2) The buckling stress obtained from the experiments was 1.8 times greater than the theoretical values for members with $\lambda > \Lambda$ and 1.5 times greater for member with $\lambda < \Lambda$. It is considered that this effect is probably in response to some existing bending stiffness in the connections. As a result, the effective member slenderness ratio, for this kind of aluminum truss system, is predicted to correspond to 0.7 times the calculated ratio assuming the unsupported length L_K to be the distance between the grids.

3) Two analytical methods for the elasto-plastic buckling analysis of the space grid structure (method A; the beam-column element model and method B; the pin-ended truss element model) were performed to investigate the possibility of predicting the buckling load and the load-displacement curves. The analytical method A and B showed both good agreement with the experimental results for the maximum buckling load and the unloading paths after buckling.

4) The collapse analysis for the actual large scale space grid was executed using analytical method B and qualitative results were obtained. The analysis results were evaluated as being suitable for practical usage in structural design.

5) This implies that the buckling behavior of space grid structures with a large number of members and joints may be simulated efficiently and rapidly on small computers using analytical method B.

References

El-Sheikh, A. (1998), "Design of space truss structures", *Structural Engineering and Mechanics*, **6**(2), 185-200.
Eurocode 9 (1997): Design of aluminum structures, Apr.
Hagginbotham, A.B. and Hanson, R.D. (1976), "Axial hysteretic behavior of steel members", *Journal of Structural Division*, **102**(ST7), 1365-1381, July.
Hiyama, Y., Takashima, H., Iijima, T. and Kato, S. (1997), "Experiments and analyses of aluminum single layered reticular domes", *IASS International Symposium*, 307-316, Nov., Singapore.
Ishikawa, K. and Kato, S. (1997), "Elastic-plastic dynamic buckling analysis of reticular domes subjected to earthquake motion", *International Journal of Space Structures*, **12**(3), 205-215.
Kahn, L.F. and Hanson, R.D. (1976), "Inelastic cycles of axially loaded steel members", *ASCE*, ST5, 947-959, May.
Kato, S. and Murata, M. (1997), "Dynamic elasto-plastic buckling simulation system for single layer reticular domes with semi-rigid connections under multiple loadings", *International Journal of Space Structures*, **12**(3), 161-172.
Mezzina, M., Prete, G. and Tosto, A. (1975), "Automatic and experimental analysis for a model of space grid in elasto-plastic behavior", *Proceedings of the Second International Conference on Space Structures*, University of Surrey, Guildford.
Saka, T. and Heki, K. (1984), "The effects of joints on the strength of space trusses", *Proceedings of the Third International Conference on Space Structures*, Edited by H. Nooshin, 417-422, September.
Schmidt, L.C. and Gregg, B.M. (1980), "A method for space truss analysis in the post-buckling range", *International Journal for Numerical in Engineering*, **15**, 237-247.
Ueki, T., Mukaiyama, Y., Shomura, M. and Kato, S. (1991), "Loading test and elasto-plastic buckling analysis of a single layer latticed dome (in Japanese)", *Transactions of AIJ*, 117-128, Mar.